



NPS61-80-016

LEVEL

2

# NAVAL POSTGRADUATE SCHOOL Monterey, California

ADA 087097



DTIC  
ELECTE  
JUL 25 1980

### TECHNICAL REPORT

Verification of the Bulk Model for  
Calculations of the Overwater Index of  
Refraction Structure Function,  $C_N^2$

K.L. Davidson and G.E. Schacher  
Environmental Physics Group

C.W. Fairall and D.E. Spiel  
BDM Corporation

E.C. Crittenden, Jr. and E.A. Milne  
Optical Propagation Group

July 1980

Approved for public release; distribution unlimited

Prepared for:  
Naval Environmental Prediction Research Facility  
Monterey, California 93940

80 7 24 030

DDG FILE COPY

NAVAL POSTGRADUATE SCHOOL  
Monterey, California


Rear Admiral J. J. Ekelund  
Superintendent


J. R. Borsting  
Provost


The work reported herein was supported in part by the Naval Environmental Prediction Research Facility, Monterey, California.

Reproduction of all or part of this report is authorized.

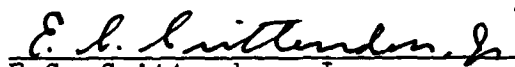
This report was prepared by:


  
K. L. Davidson  
Associate Professor of Meteorology

  
G. E. Schacher  
Professor of Physics


  
C. W. Fairall  
BDM Corporation

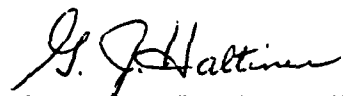
  
D. E. Spier  
BDM Corporation

  
E. C. Crittenden, Jr.  
Professor of Physics

  
E. A. Milne  
Professor of Physics

Approved by:

  
J. W. DYER, Chairman  
Department of Physics and Chemistry

  
G. J. Haltiner, Chairman  
Department of Meteorology

  
William M. Tolles  
Dean of Research

UNCLASSIFIED

SECURITY CLASSIFICATION OF THIS PAGE (When Data Entered)

REPORT DOCUMENTATION PAGE		READ INSTRUCTIONS BEFORE COMPLETING FORM
1. REPORT NUMBER 14) NPS-61-80-016	2. GOVT ACCESSION NO. AD-A087097	3. RECIPIENT'S CATALOG NUMBER
4. TITLE (and Subtitle) 6) Verification of the Bulk Model for Calculations of the Overwater Index of Refraction Structure Function, $C_N^2$ , NL		5. TYPE OF REPORT & PERIOD COVERED 9) Technical Report
7. AUTHOR(s) 10) K.L. Davidson, G.E. Schacher, C.W. Fairall, D.E. Spiel, E.C. Crittenden Jr. and E.A. Milne		6. PERFORMING ORG. REPORT NUMBER
9. PERFORMING ORGANIZATION NAME AND ADDRESS Department of Physics & Chemistry Naval Postgraduate School Monterey, CA 93940		8. CONTRACT OR GRANT NUMBER(s)
11. CONTROLLING OFFICE NAME AND ADDRESS Naval Environmental Prediction Research Facility Monterey, CA 93940		10. PROGRAM ELEMENT, PROJECT, TASK AREA & WORK UNIT NUMBERS 11)
14. MONITORING AGENCY NAME & ADDRESS (if different from Controlling Office) 15) 1451		12. REPORT DATE Jul 1980
		13. NUMBER OF PAGES 42
		15. SECURITY CLASS. (of this report) Unclassified
		15a. DECLASSIFICATION/DOWNGRADING SCHEDULE
16. DISTRIBUTION STATEMENT (of this Report) Distribution Unlimited		
17. DISTRIBUTION STATEMENT (of the abstract entered in Block 20, if different from Report) 21-F		
18. SUPPLEMENTARY NOTES		
19. KEY WORDS (Continue on reverse side if necessary and identify by block number) Refraction structure function, bulk model, optical propagation IC overwater		
20. ABSTRACT (Continue on reverse side if necessary and identify by block number) Overwater measurements of mean and fluctuating meteorological parameters have been made coincident with optical scintillation measurements. These data have been used to verify the NPS bulk aerodynamics model for calculating the index of refraction structure function, $C_N^2$ . The average disagreement between calculated and measured values was 33% verifying the validity of the model. IR measured sea surface temperatures cannot be used in the model and this is discussed.		

DD FORM 1 JAN 73 1473

EDITION OF 1 NOV 68 IS OBSOLETE  
S/N 0102-014-660

UNCLASSIFIED

SECURITY CLASSIFICATION OF THIS PAGE (When Data Entered)

25-1450

Verification of the Bulk Model for Calculations of the Overwater  
Index of Refraction Structure Function,  $C_N^2$

K.L. Davidson and G.E. Schacher, Environmental Physics Group  
C.W. Fairall and D.E. Spiel, BDM Corporation  
E.C. Crittenden, Jr. and E.A. Milne, Optical Propagation Group  
Naval Postgraduate School  
Monterey, California 93940

Overwater measurements of mean and fluctuating parameters have been made coincident with optical scintillation measurements. These data have been used to verify the NPS bulk aerodynamic model for calculating the index of refraction structure function,  $C_N^2$ . The average disagreement between calculated and measured values was 33% verifying the validity of the model. IR measured sea surface temperatures cannot be used in the model and this is discussed.

Accession For	
NTIS GRA&I	<input checked="" type="checkbox"/>
DDC TAB	<input type="checkbox"/>
Unannounced	<input type="checkbox"/>
Justification	
By _____	
Distribution/_____	
Availability Codes	
Dist	Avail and/or special
A	

## OUTLINE

I. Introduction	5-6
II. Experimental Arrangement	7-13
III. Bulk Model	14-20
IV. Comparison with Optical Measurements	21-27
V. Thermal Turbulence Measurements	28-32
VI. Bulk Model with IR Sea Surface Temperature	33-37
VII. Conclusions	38-42

## TABLES

Table 1. Shipboard meteorological data

Table 2.  $c_{DN}$  vs wind speed at 10 m from Kondo

Table 3. Calculated scaling parameters and index of refraction  
structure function

## FIGURES

- Figure 1. Experimental Area
- Figure 2.  $C_N^2$ -optics vs  $C_N^2$ -bulk using bulk measured sea surface temperature. Solid line is perfect agreement, dashed lines are factor of two disagreement.
- Figure 3. Aircraft measured IR sea surface temperature and  $C_T^2$  vs distance from shore. Optical path location is shown by a vertical dark line.
- Figure 4.  $C_N^2$ -optics vs  $C_N^2$ -turbulence, data not corrected for salt incrustation. Solid line is perfect agreement, dashed lines are a factor of two disagreement.
- Figure 5.  $C_N^2$ -optics vs  $C_N^2$ -turbulence, data corrected for salt encrustation. Solid line is perfect agreement, dashed lines are factor of two disagreement.
- Figure 6.  $C_N^2$ -optics vs  $C_N^2$ -bulk using IR measured sea surface temperature. Solid line is perfect agreement, dashed lines are factor of two disagreement.
- Figure 7. Difference in measured sea surface temperatures (IR-bulk) vs time. Shaded areas indicate cloud cover.

## I. INTRODUCTION

Surface layer turbulence models have been improved to the point where quite good estimates of turbulence intensities can be made from readily measured meteorological parameters (wind, temperature, and humidity). However, applications of present formulations to estimate turbulent intensities of the optical index of refractions within the surface layer have been limited by acknowledged deficiencies. These are the

1. bulk scaling of the contributions of the turbulent variance of water vapor and the turbulent covariance of water vapor and temperature.
2. observational verification of the role of turbulence on overwater optical degradation based on both optical measurements and model estimates of  $C_N^2$ , the refractive index structure function parameter.

The purpose of this report is to describe combined overwater measurements that allow a comparison of optical measured values of  $C_N^2$  with values calculated from both turbulence and bulk measurements. The turbulence estimates include contributions from both variance ( $C_T^2$  and  $C_q^2$ ) and covariance ( $C_{Tq}$ ) components. The bulk model is that formulated by the Naval Postgraduate School (NPS) and utilizes stability corrected scaling parameters. As will be shown here the bulk formulation yields results which are considerably better than direct turbulence measurements and are in good agreement with optical measurements.

In order to meet the above needs the Naval Environmental Prediction Research Facility and NPS planned a series of coincident optical and meteorological measurements to be made on Monterey Bay. This work was undertaken during the Marine Aerosol Generation and Transport (MAGAT) experiment. The work was performed from 28 April to 9 May 1980 by the Environmental Physics Group of NPS in cooperation with the NPS Optical Propagation Group and Airborne Research Associates (ARA). The purpose of the effort was to verify overwater optical propagation models that have been developed to predict extinction and scintillation. The purpose of this report is to evaluate the bulk aerodynamic method for obtaining the index of refraction structure function from mean meteorological parameters. Evaluation of the NPS boundary layer aerosol model will be the subject of another report.

During MAGAT, the full range of meteorological measurements were made on the RV/ACANIA and on the ARA aircraft. This included both mean and fluctuating parameters. All model evaluations in this report were made using the shipboard data. Optical measurements were made on the 13 km overwater range, at regular periods around the clock for eight days in order to experience as wide a range of conditions as possible. The ship was stationed on the optical path frequently for direct comparison with the optical measurements.

## II. EXPERIMENTAL ARRANGEMENT

The RV/ACANIA was equipped with a multi-level measurement system to measure both mean and fluctuating meteorological parameters. The heights at which sensors were placed above mean sea level and the quantities measured are shown in Table 1:

TABLE 1. Shipboard Measurement Configuration

<u>Height</u>	<u>Parameters Measured</u>
0	Sea surface IR temperature ( $T_{IR}$ ) Bulk water temperature ( $T_S$ )
4.2 m	Mean temperature ( $T$ ) Mean wind speed ( $U$ ) Wind speed fluctuation ( $U'$ )
7.0 m	Mean temperature Mean wind speed Mean dew point ( $T_D$ ) Temperature fluctuation ( $T'$ ) Wind speed fluctuation Humidity fluctuation ( $H'$ )
19.6 m	Mean temperature Mean wind speed Mean wind direction ( $WD$ ) Mean humidity Wind speed fluctuation

In addition to these sensors, the visibility (V) and inversion height ( $Z_i$ ) were determined and aerosol spectra were measured at a height of 8.5 m.

The sensors used were:

$T_{IR}$	Barnes PRT-5
$T_S, T$	Rosemount platinum thermometers mounted in Gill aspirators
U, WD	MRI 1022 system
$T_D$	General Eastern cooled mirror
$T'$	2.5 $\mu$ platinum microthermal sensors and Sylvania 140 bridge
U'	60 $\mu$ platinum on quartz substrate and TSI 1054 bridge
H'	ERC Lyman-Alpha
$Z_i$	Aerovironment 300 Sounder
V	MRI 1580 Fog Visicometer

Two  $T'$  sensors, placed a distance of 30 cm apart, were the primary sensors for determining  $C_T^2$ . A single  $T'$  sensor was placed immediately adjacent to the active volume of the Lyman-Alpha in order to measure the temperature-humidity cospectrum. The temperature measurement circuitry in the dew point sensor was not used due to instability problems. This system has a platinum sensor mounted in a three wire configuration. The leads were changed to 4 wire to improve the accuracy and the same system was then used to measure all of the temperatures  $T_S, T$  and  $T_D$ .

The IR thermometer was mounted on a railing on the ship approximately 4 m above the water. The sensor was angled at approximately 45° to insure that the ship wake was not included in the field of view. The platinum thermometer was inserted in a brass plug in the end of a long 1" diameter tygon tube. The arrangement was slightly less buoyant than desired and floated so that it averaged the water temperature for about the first 12" below the surface. The depth depended on the ship speed.

All data were recorded with a Hewlett Packard 3052 data acquisition system controlled by a Hewlett Packard 9825S computer. Almost all data were obtained as one half hour averages. The same voltmeter was used to measure voltages and the 4-wire resistances.

Neither descriptions of the optical measurements system<sup>(1)</sup> nor presentation of the resulting data<sup>(2)</sup> will be given here as they are included in another report. Figure 1 shows the location of the measurement area in Monterey Bay. The optical path is located so that it is approximately perpendicular to the prevailing northwest flow in such a location that land influence is minimal. Also, scintillation measurements weight the center of the path further reducing any land influence. For most of the measurements reported here the ship was anchored at the position shown in the figure; a few measurements were made while the ship was in motion within the square area shown. When anchored, the ship automatically faced into the wind and while underway, data was only taken when the ship was headed into the wind.

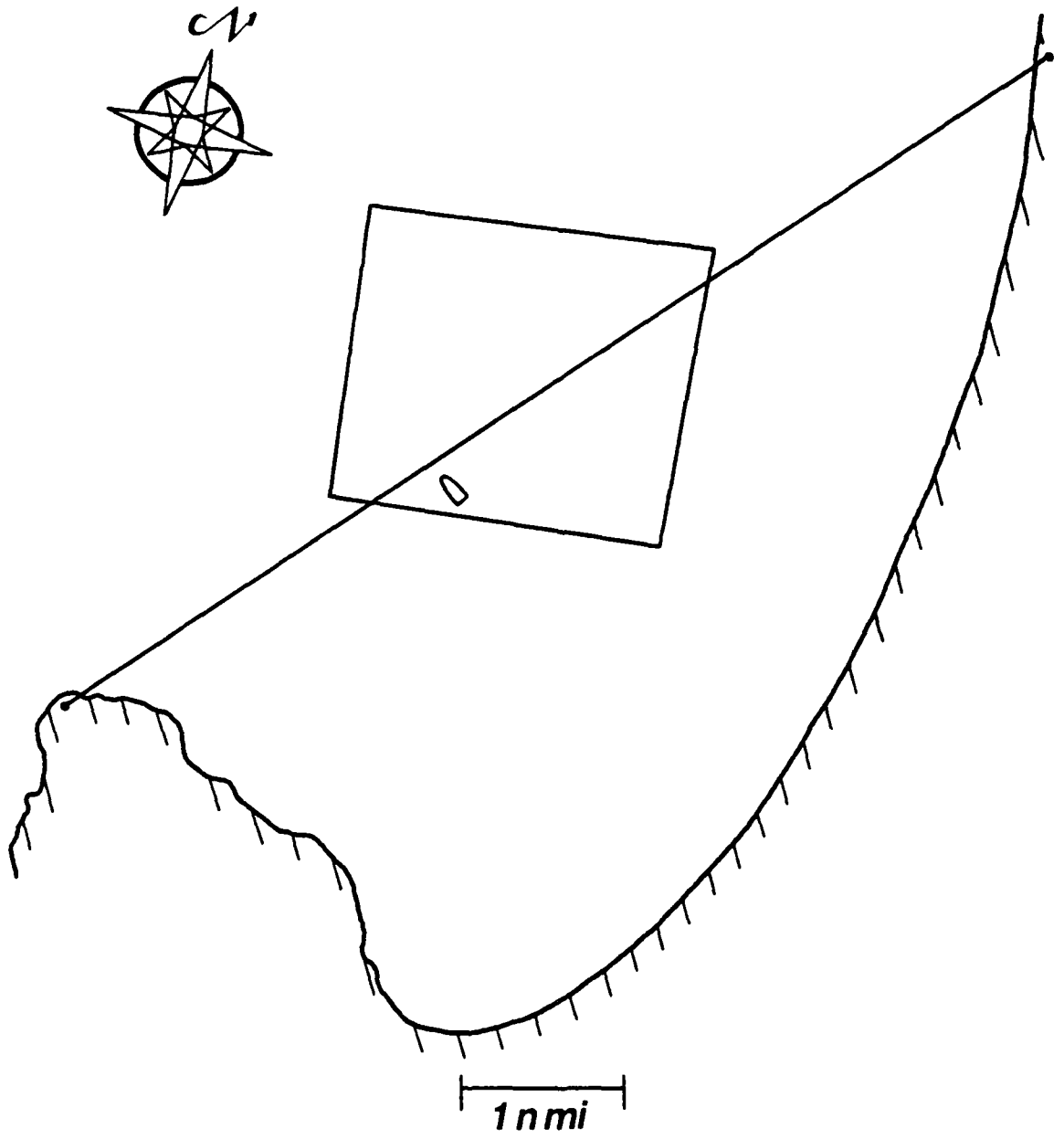


Figure 1

The ship system measures the properties of the air that passes its location during a one half hour period. The optical path averages the properties of the air over the 13 km path length. We are thus comparing a time average and a space average. Or, if there is horizontal homogeneity along the mean wind direction, the time average taken at the ship is equivalent to a space average along the mean wind. In any event, the two averages obtained by the optical technique and by the meteorological measurements are not exactly equivalent. Exactly how this affects comparisons of optical and meteorological results cannot be determined without detailed knowledge of the local airflow and temperature patterns. This topic is now under investigation.

Table 1 lists the meteorological data that was acquired coincident with optical scintillation measurements. Listed are the true wind speed, sea temperature from both bulk and IR thermometers, air temperature, relative humidity, and the calculated stability parameter  $Z/L$ .

COUNT	DATE	TIME	U	TS	Tir	T	H	Z/L	
1	04/27-1931	2211	2.59	14.38	12.70	13.49	90.06	-.675	Non
2	04/29-0614	523	8.26	13.95	12.85	12.68	85.95	-.073	Equilibrium
3	04/29-0644	639	8.70	13.98	12.85	12.59	85.37	-.065	"
4	04/29-0714	717	8.52	13.96	12.83	12.43	85.44	-.081	"
5	04/29-0744	759	8.15	13.92	12.81	12.37	84.82	-.091	"
6	04/29-0834	835	6.86	13.87	12.77	12.22	85.40	-.142	"
7	04/29-0904	908	6.83	13.83	12.72	12.37	84.18	-.131	"
8	04/29-1012	1023	4.81	13.81	12.65	12.53	82.98	-.261	"
9	05/01-2337	2224	2.26	13.15	11.05	13.64	84.39	.318	
10	05/02-0527	520	2.13	13.25	11.22	12.53	94.19	-.738	
11	05/02-0642	644	1.12	13.21	11.54	12.30	95.37	-2.847	
12	05/02-0734	742	4.14	13.13	11.92	12.40	92.63	-.191	
13	05/02-0839	841	4.35	13.07	11.90	12.18	91.15	-.208	
14	05/02-0909	902	3.31	13.08	11.83	12.24	90.89	-.362	
15	05/02-0939	949	2.06	13.11	11.41	12.28	90.36	-.977	
16	05/02-1048	1054	1.19	13.44	10.61	11.95	93.61	-4.259	
17	05/02-1218	1224	2.77	13.97	10.99	12.43	92.06	-.976	
18	05/02-1318	1322	6.05	13.59	11.10	12.62	90.44	-.108	
19	05/02-1418	1429	6.64	13.57	11.26	12.66	90.71	-.082	
20	05/02-1653	1645	5.59	13.41	11.89	12.60	89.94	-.112	
21	05/02-1723	1721	5.17	13.41	12.06	12.46	90.33	-.153	
22	05/02-1853	1841	4.39	13.44	12.22	12.28	90.77	-.266	
23	05/02-1923	1927	4.43	13.40	12.26	12.40	90.34	-.228	
24	05/03-2355	2342	4.10	13.58	12.02	12.59	90.55	-.265	
25	05/04-0014	210	4.38	13.42	11.80	12.68	92.26	-.164	
26	05/04-0050	50	2.25	13.19	12.12	12.45	92.62	-.704	
27	05/04-0142	125	4.07	13.46	12.23	12.55	93.76	-.235	
28	05/04-2311	2259	5.78	14.10	12.27	12.61	95.05	-.174	Non
29	05/04-2317	2321	5.98	13.79	12.13	12.64	95.14	-.123	Equilibrium
30	05/04-2346	2326	5.94	14.26	12.51	12.49	93.37	-.201	"
31	05/05-0009	2348	5.93	13.98	12.17	12.49	92.71	-.171	"
32	05/05-0016	17	3.39	13.70	11.91	12.40	91.47	-.539	"
33	05/05-0059	50	2.99	13.78	12.08	12.40	91.83	-.742	"
34	05/05-0137	128	2.91	13.40	11.83	12.32	93.16	-.598	"
35	05/05-0238	239	2.09	13.65	12.21	12.60	88.44	-1.229	"
36	05/05-0257	256	3.45	13.70	12.02	12.62	88.27	-.449	"
37	05/05-1925	1922	11.61	13.47	11.60	13.90	89.72	.011	
38	05/05-1955	1948	11.96	13.38	11.58	13.97	87.56	.011	
39	05/08-1804	1805	11.05	13.22	11.65	12.59	83.38	-.022	
40	05/08-1834	1837	10.32	13.12	11.78	12.47	83.62	-.024	

Table 1. Shipboard Meteorological Data

COUNT	DATE	TIME	U	TS	Tip	I	Q	Δ/L
41	05/09-1920	1927	9.50	13.92	12.15	13.11	85.14	-.032
42	05/08-2031	2040	6.22	13.93	12.52	13.06	85.33	-.096
43	05/09-0919	918	6.65	14.05	12.71	13.75	89.29	-.033
44	05/09-0942	941	7.40	14.05	12.78	13.74	83.79	-.026
45	05/09-1012	1019	6.68	14.15	12.68	14.00	86.21	-.017
46	05/09-1118	1116	7.18	14.30	12.76	14.62	84.86	.013
47	05/09-1148	1147	7.56	14.37	12.80	14.67	84.17	.012
48	05/09-1158	1200	8.26	14.36	12.88	14.78	84.45	.018

Non  
Equilibrium

Table 1 Con't.

### III. BULK MODEL

The bulk model uses the differences in the values of mean parameters between the surface and a reference height to estimate small scale properties of the atmosphere. This NPS bulk model was first developed in 1977 to calculate the index of refraction structure function,  $C_N^2$ , and was first applied to evaluate results from the CEWCOM-78 experiment(3). Since that time, NPS has verified the overwater scaling and stability correction functions for wind, temperature, and humidity. The model has proven to work quite well for predicting small scale fluctuations in wind, temperature, and water vapor as was shown by comparing direct fluctuation measurements with the bulk calculated values.(4,5,6) The CEWCOM-78 report contains a sketch of the model and the full development is presented below.

The optical refractive-index structure function parameter is related to the temperature structure function parameter,  $C_T^2$ , and the humidity structure function parameter,  $C_Q^2$ , by (7)

$$C_N^2 = (79 \times 10^{-6} P/T^2)^2 (C_T^2 + .113 C_{TQ} + 3.1 \times 10^{-3} C_Q^2) \quad (1)$$

Where P is the pressure in mb and T is the absolute temperature.  $C_{TQ}$  is the temperature-humidity cospectral structure function.

#### A. Monin-Obukhov Scaling

$C_x^2$  can be related to the measured meteorological quantities through Monin-Obukhov surface layer similarity parameters(8,9)

$$C_T^2 = T_*^2 z^{-2/3} f(\xi), \quad (2a)$$

$$C_Q^2 = Q_*^2 z^{-2/3} A f(\xi), \quad (2b)$$

where  $T_*$  is the potential temperature scaling parameter,  $Q_*$  is the water vapor density scaling parameter ( $\text{gm}/\text{m}^3$ ),  $Z$  is the height above the surface,  $\xi = Z/L$  is the similarity (dimensionless) height parameter and  $f(\xi)$  is the empirical function found by Wyngaard, et al. The quantity  $A$  is a constant approximately equal to 0.8.(5) The cospectral function is given by

$$C_{TQ} = r_{TQ} T_* Q_* Z^{-2/3} A^{1/2} f(\xi). \quad (2c)$$

where  $r_{TQ}$  is the temperature-humidity correlation parameter equal to 0.8 under unstable conditions. The value of  $r_{TQ}$  for stable conditions is not well known in the surface layer. Note that  $Q_*$  in ( $\text{gm}/\text{m}^3$ ) and  $q_*$  in ( $\text{gm}/\text{kg}$ ) are related by  $Q_* = 1.3 q_*$  at the surface.  $q_*$  is the water vapor mixing ratio scaling parameter. The Monin-Obukhov length scale,  $L$ , is defined by

$$L = (T/kg) U_*^2 [T_* + 6.1 \times 10^{-4} Tq_*]^{-1}, \quad (3)$$

where  $k$  is von Karman's constant (0.35),  $g$  is the acceleration of gravity, and  $U_*$  is the friction velocity.

The problem of predicting  $C_N^2$  is now reduced to finding values for  $q_*$ ,  $T_*$  and  $\xi$  (or  $L$ ). The bulk method is based on obtaining values of temperature, relative humidity, and wind speed at the sea surface and at some reference height,  $Z$ . The difference between the surface value and the value at height  $Z$  can be related to the scaling parameter through the profile equations.(10)

$$U_* = kU [\ln Z/Z_0 - \psi_1(\xi)]^{-1}, \quad (4a)$$

$$T_* = (T - T_S) \alpha_T k [\ln Z/Z_{0T} - \xi_2(\xi)]^{-1} \quad (4b)$$

$$q_* = (q - q_S) \alpha_T k [\ln Z/Z_{0T} - \xi_2(\xi)]^{-1} \quad (4c)$$

where  $\alpha_T$  is the ratio of heat transfer to momentum transfer at  $\xi = 0$ , and  $\xi$  is the value at height  $Z$ .<sup>(11)</sup> Businger, et al. found  $\alpha_T = 1.35$ , others have found different values. The quantities  $Z_0$  and  $Z_{0T}$  are the roughness lengths for velocity and temperature profiles. Note that these equations can be written in the standard drag coefficient form

$$U_* = c_D^{1/2} U, \quad (5a)$$

$$T_* = c_T^{1/2} (T - T_S), \quad (5b)$$

$$q_* = c_T^{1/2} (q - q_S). \quad (5c)$$

In Eqs. 4 and 5, we have assumed that the water vapor dependences ( $q$ ) can be treated with the same coefficients as the temperature ( $Z_{0T}$ ,  $c_T$ ).

The stability dependence of the drag coefficients can be obtained from Eqs. 4 and 5

$$c_D^{1/2} = (k/\ln Z/Z_0)[1 - (\ln Z/Z_0)^{-1} \psi_1(\xi)]^{-1} \quad (6a)$$

$$c_T^{1/2} = (\alpha_T k / \ln Z/Z_{0T}) [1 - (\ln Z/Z_{0T})^{-1} \psi_2(\xi)]^{-1} \quad (6b)$$

We can define the neutral stability drag coefficients in terms of the roughness lengths as

$$c_{DN}^{1/2} = k(\ln Z/Z_0)^{-1}, \quad (7a)$$

$$c_{TN}^{1/2} = \alpha_T k (\ln Z/Z_{0T})^{-1} \quad (7b)$$

Note that the given drag coefficient at height  $Z$ , one can calculate the roughness length

$$Z_0 = Z \exp[-k/c_{DN}^{1/2}] \quad (8a)$$

$$Z_{0T} = Z \exp[-\alpha_T k/c_{TN}^{1/2}] \quad (8b)$$

We are now able to calculate the atmospheric stability at height  $Z$ ,  $\xi = Z/L$ , using Eqs. 3, 4 and 7,

$$\xi = \xi_0 [1 - (\ln Z/Z_0)^{-1} \psi_1(\xi)]^2 [1 - (\ln Z/Z_{0T})^{-1} \psi_2(\xi)] \quad (9)$$

where

$$\xi_0 = (kgZ/T) (c_{TN}^{1/2}/c_{DN}) (\Delta T + 6.1 \times 10^{-4} T\Delta q) U^{-2} \quad (10)$$

### B. Empirical Constants and Quantities

We have been using a value of von Karman's constant  $k = 0.35$  based on the original Businger, et al. work. Recently, Garratt<sup>(12)</sup> has published a survey which implies  $k = 0.41$ . Businger, et al.<sup>(11)</sup> found  $\alpha_T = 1.35$ , however, if one uses  $k = 0.41$  then a value of  $\alpha_T = 1.15$  would maintain a constant  $\alpha_T k$ .

A typical value of  $c_{DN}$  at  $Z = 10$  m is  $1.3 \times 10^{-3}$  which yields  $Z_0 = 6 \times 10^{-4}$  m. Kondo<sup>(13)</sup> and Garratt<sup>(12)</sup> both give equations for wind speed dependence of the  $Z = 10$  m drag coefficient. Kondo's formulae are used in our model formulation and are given in Table 1.

Table 2.  $c_{DN}$  versus wind speed at 10 m from Kondo<sup>(13)</sup>.

<u>U(ms<sup>-1</sup>)</u>	<u><math>c_{DN} \times 10^3</math></u>
.3 - 2.2	$1.08 \times U^{-.15}$
2.2 - 5.0	$.77 + .086 \times U$
5.0 - 8.0	$.87 + .067 \times U$
8.0 - 25.0	$1.2 + .025 \times U$

The temperature drag coefficient has been measured by several groups (see Davidson, et al.<sup>(4)</sup>, for a summary), but we feel a best estimate is  $c_{TN} = 1.3 \times 10^{-3}$  at  $Z = 10$  m. Assuming  $\alpha_T = 1.35$ , we obtain  $Z_{0T} = 2.0 \times 10^{-5}$  m. For our bulk model, we assume that  $Z_{0T}$  is independent of wind speed and that the wind speed dependence of  $Z_0$  can be obtained from Kondo's  $c_{DN}$  using Equ. 8a with  $Z = 10$  m.

### C. Procedure

1. Input data are sea surface temperature ( $T_S$ ), air temperature ( $T$ ), relative humidity or dew point ( $H$  or  $T_D$ ) and wind speed ( $U$ ). The last three are measured at a reference height  $Z$ . From  $T$  and  $H$  (or  $T_D$ ) calculate  $q$ . From  $T_S$  calculate  $q_S$  assuming that  $H = 100\%$  at the surface.

2. From  $U$ , calculate  $c_{DN}$  (Kondo) for  $Z = 10$  m

From  $c_{DN}$ ,  $Z = 10$ , calculate  $Z_0$  (Equ. 8a)

Let  $Z_{0T} = 2.0 \times 10^{-5}$

Let  $c_{TN} = 1.3 \times 10^{-3}$  if  $Z = 10$  m. If  $Z \neq 10$  m, use Eqs. 7a and 7b to calculate the drag coefficients.

3. From  $\Delta T = T - T_S$  (potential temperature)

$$\Delta q = q - q_S$$

$$\Delta U = U, \text{ calculate } \xi_0 \text{ (Equ. 10)}$$

4. Solve Equ. 9 iteratively to obtain  $\xi$  from  $\xi_0$ . Note that  $L = Z/\xi$ .

5. From  $T^*$ ,  $Q^* = 1.3 q^*$ , and  $Z/L$  calculate  $C_T^2$ ,

$C_Q^2$  and  $C_{TQ}$  at any height using Equ. 2.

Calculate  $C_N^2$  from Equ. 1.

D. Stability Correction Functions

Velocity Profile:

$$\psi_1(\xi) = 2 \ln [(1 + x)/2] + \ln [(1 + x^2)/2] - 2 \tan^{-1}(x) + \pi/2 \quad \xi < 0$$

$$x = (1 - 15\xi)^{1/4}$$

$$\psi_1(\xi) = -4.7\xi \quad \xi > 0$$

Temperature Profile:

$$\psi_2(\xi) = 2 \ln [(1 + x)/2] \quad \xi < 0$$

$$x = (1 - 9\xi)^{1/2}$$

$$\psi_2(\xi) = -6.5\xi \quad \xi > 0$$

#### IV. COMPARISON WITH OPTICAL MEASUREMENTS

Table 3 presents the following computed quantities: (1) scaling parameters for wind, temperature and water vapor, (2)  $C_N^2$  from turbulence measurements, (3)  $C_N^2$  from the bulk model, (4) the optically measured  $C_N^2$  and, for reference, the stability parameter.

Comparisons of  $C_N^2$  calculated from the bulk model with those measured optically are shown in Figure 2. The solid points are for cases where the surface layer is in equilibrium and the open circles are for non-equilibrium, which will be explained below. The solid line indicates perfect agreement and the two dashed lines are for a factor of two disagreement. For all but two of the eighteen cases where the surface layer was in equilibrium the agreement is within a factor of two. The mean percent error, taking the optical value to be correct, for all equilibrium values is 33%. This is very good agreement.

We have found that at times, there is a change in water temperature in Monterey bay in the vicinity of the optical beam. The change is from colder to warmer as the shore is approached. As implied above, the change in temperature is not always present and the frequency of occurrence has not been determined. Figure 3 shows a plot of sea surface temperature vs position measured by the ARA aircraft using an IR thermometer. The aircraft flew a course perpendicular to the optical path from the shore to 25 km at sea. The location of the optical path is shown in the figure by a heavy vertical line. The water temperature is seen to gradually increase (but not monotonically) by a few tenths of a

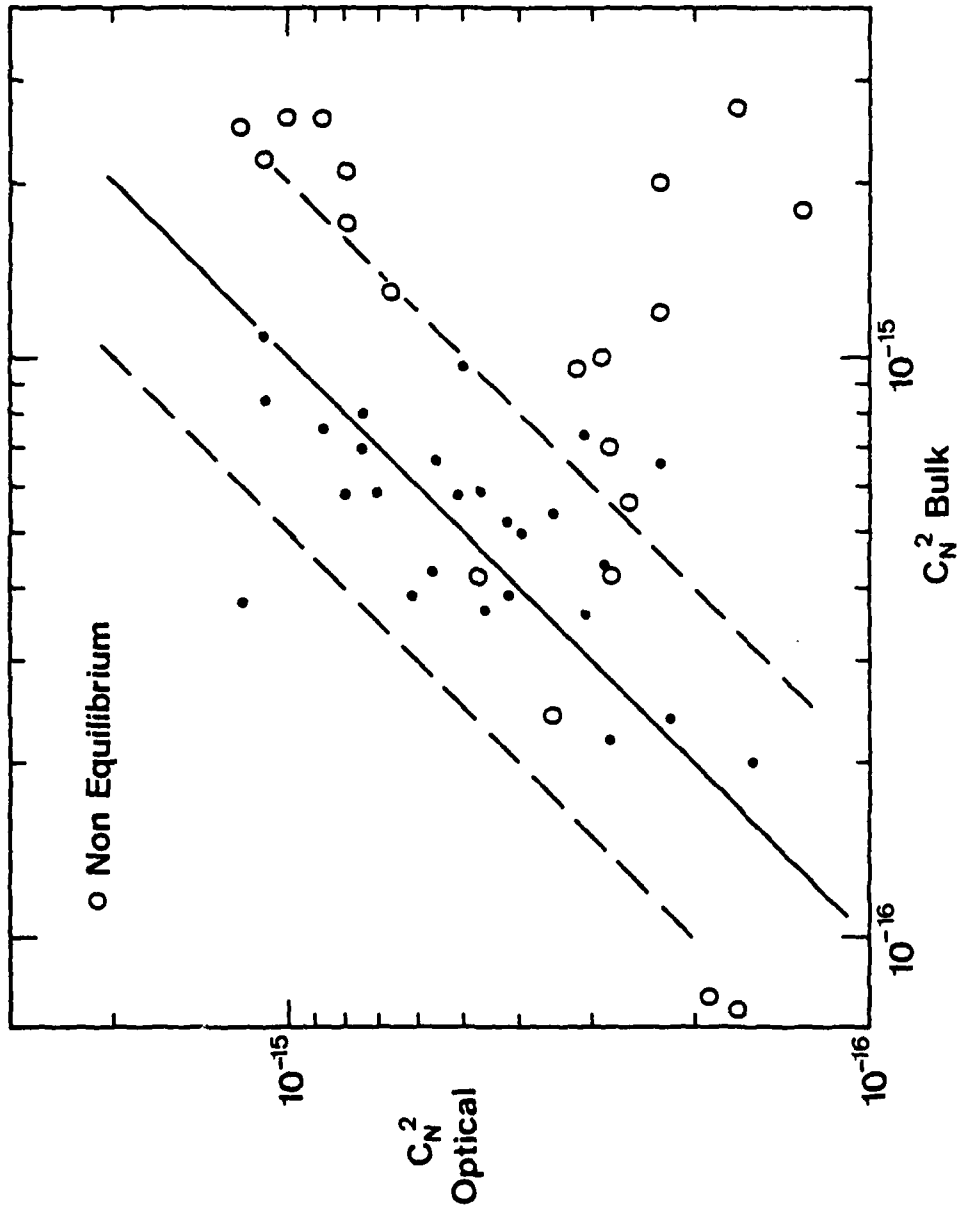


Figure 2

THIS PAGE IS UNCLASSIFIED  
EXCEPT WHERE SHOWN OTHERWISE

MODE	DATE	Z/L	0F	1F	q*	CN2_0P1	CN2_TURB	CN2_MODEL
1	04/27-1731	-.675	.083	-.028	-.058	3.1E-16	3.1E-16	3.6E-16
2	04/29-0614	-.073	.294	-.039	-.079	8.0E-16	1.9E-15	1.7E-15
3	04/29-0644	-.065	.327	-.044	-.084	1.1E-15	1.7E-15	2.2E-15
4	04/29-0714	-.081	.306	-.049	-.086	1.0E-15	1.7E-15	2.6E-15
5	04/29-0744	-.091	.291	-.049	-.088	1.2E-15	2.0E-15	2.5E-15
6	04/29-0834	-.142	.240	-.053	-.088	8.8E-16	1.5E-15	2.6E-15
7	04/29-0904	-.131	.238	-.047	-.088	8.0E-16	3.0E-15	2.1E-15
8	04/29-1012	-.261	.161	-.041	-.091	6.7E-16	1.9E-15	1.3E-15
9	05/01-2337	.318	.058	.015	-.037	2.9E-16	7.2E-16	4.4E-16
10	05/02-0527	-.738	.068	-.022	-.037		1.6E-16	2.1E-16
11	05/02-0642	-2.847	.041	-.033	-.041	1.6E-16		2.0E-16
12	05/02-0734	-.190	.134	-.021	-.041	4.6E-16		3.7E-16
13	05/02-0839	-.208	.143	-.027	-.050	4.7E-16	8.1E-16	5.9E-16
14	05/02-0909	-.367	.106	-.026	-.050	5.6E-16	7.8E-16	4.3E-16
15	05/02-0939	-.977	.067	-.027	-.055	1.2E-15	6.2E-16	2.8E-16
16	05/02-1048	-4.257	.044	-.059	-.065	8.0E-16	8.5E-16	4.9E-16
17	05/02-1218	-.976	.090	-.055	-.067	1.1E-15	1.2E-15	1.1E-15
18	05/02-1318	-.108	.206	-.029	-.055	1.1E-15	1.9E-15	8.5E-16
19	05/02-1418	-.082	.228	-.027	-.052	7.4E-16	1.2E-15	8.0E-16
20	05/02-1653	-.112	.188	-.024	-.052	7.1E-16	8.7E-16	5.9E-16
21	05/02-1723	-.153	.173	-.029	-.054	8.8E-16	1.2E-15	7.6E-16
22	05/02-1853	-.266	.145	-.037	-.057	5.0E-16	9.1E-16	9.7E-16
23	05/02-1923	-.228	.146	-.031	-.055	3.1E-16	9.2E-16	7.4E-16
24	05/02-2355	-.265	.134	-.030	-.055	2.3E-16	1.3E-15	6.6E-16
25	05/04-0014	-.164	.143	-.021	-.042	4.2E-16	2.0E-15	3.9E-16
26	05/04-0050	-.704	.071	-.022	-.043	2.8E-16	3.7E-16	2.2E-16
27	05/04-0142	-.235	.132	-.027	-.042	3.5E-16	1.1E-15	5.4E-16
28	05/04-2311	-.174	.198	-.048	-.051	1.3E-16		1.9E-15
29	05/04-2317	-.123	.204	-.036	-.042	2.3E-16		1.2E-15
30	05/04-2346	-.201	.205	-.060	-.065	1.7E-16		2.7E-15
31	05/05-0007	-.171	.204	-.049	-.059	2.3E-16		2.0E-15
32	05/05-0016	-.537	.111	-.045	-.061	2.9E-16		1.0E-15
33	05/05-0059	-.742	.097	-.048	-.061	3.2E-16		9.5E-16
34	05/05-0137	-.598	.093	-.035	-.048	2.6E-16		4.7E-16
35	05/05-0238	-1.229	.068	-.036	-.069	2.8E-16		5.2E-16
36	05/05-0257	-.449	.112	-.035	-.067	2.8E-16		7.0E-16
37	05/05-1725	.011	.432	.021	-.024	4.2E-16		5.2E-16
38	05/05-1955	.011	.446	.023	-.028	5.9E-16	2.4E-15	6.2E-16
39	05/08-1804	-.022	.418	-.016	-.096	5.8E-16	1.9E-15	5.1E-16
40	05/08-1849	-.024	.389	-.017	-.077	4.0E-16	1.9E-15	5.0E-16

Table 3. Calculated Scaling Parameters and Index of Refraction Structure Function

COUNT	DATE	Z/L	OX	T*	q*	CN2_OPT	CN2_TURE	CN2_MODEL
41	05/08-1920	-.032	.356	-.022	-.070	7.5E-16	1.9E-15	7.0E-16
42	05/08-2031	-.096	.212	-.024	-.070	5.6E-16	5.1E-16	6.6E-16
43	05/09-0919	-.033	.226	-.006	-.044	1.7E-16	2.4E-16	7.5E-17
44	05/09-0942	-.026	.255	-.006	-.046	1.9E-16	1.6E-16	7.9E-17
45	05/09-1012	-.017	.226	.002	-.050	3.5E-16	1.2E-16	
46	05/09-1118	.013	.241	.016	-.052	2.2E-16		2.4E-16
47	05/09-1148	.012	.256	.016	-.051	3.5E-16		2.4E-16
48	05/09-1158	.018	.283	.020	-.048	4.7E-16		4.2E-16

Table 3 Con't.

degree up to about 6 km from shore then increases by one degree in 4 km. The optical path is in the middle of the rapid change region on the day the profile shown was determined.

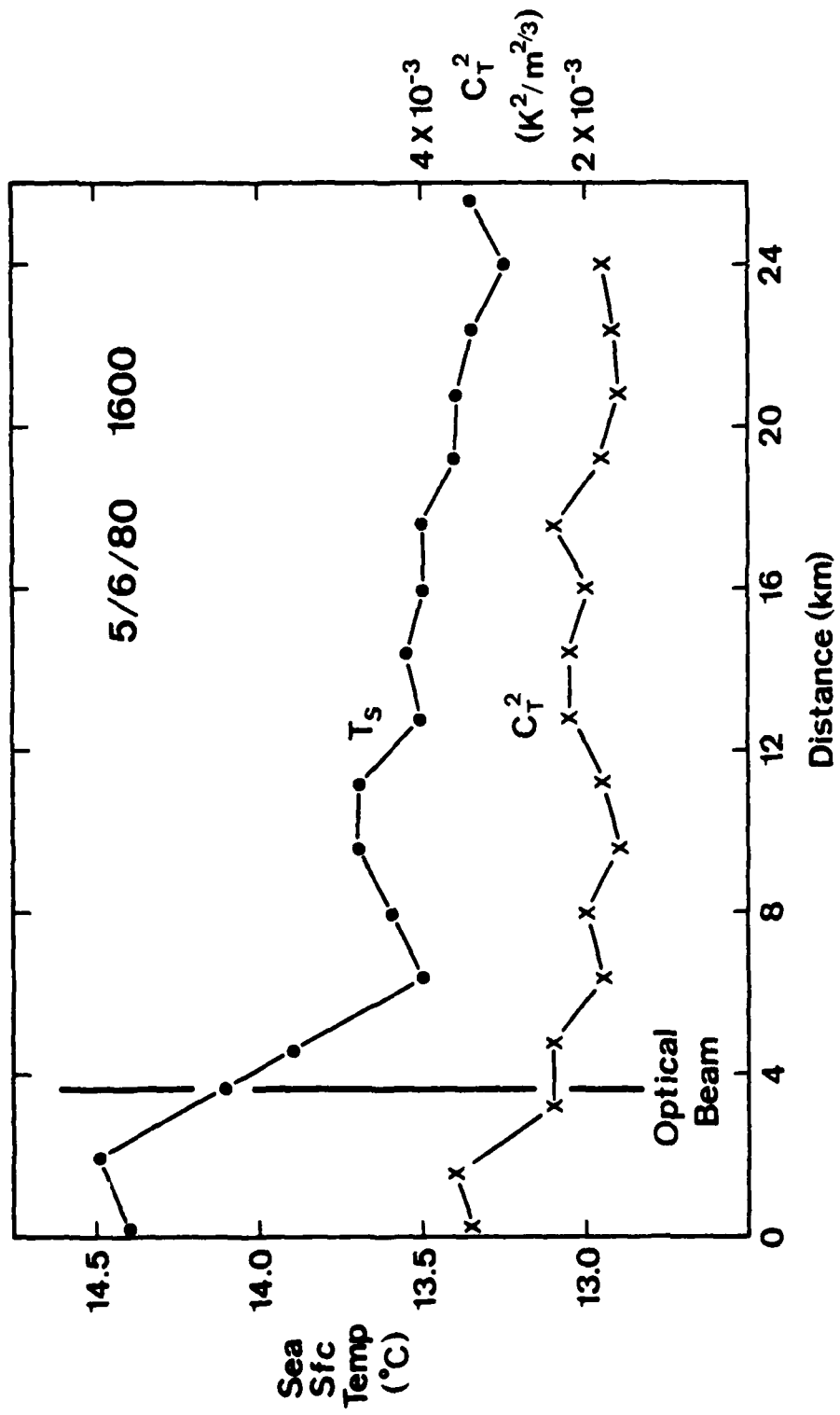
It was fairly easy to determine the days when the temperature discontinuity existed from shipboard measurements. The shipboard operation required that it move in and out of the bay frequently, so we were able to compare bay temperatures to those further at sea. On several days the bay temperature at the optical path was approximately one degree elevated. We assume that the surface layer may not be in equilibrium at the ship site when the temperature jump exists and have indicated data from such days by open circles in Figure 2. Note that during such times the optical path may also be inhomogeneous.

The results clearly demonstrate the air is not in equilibrium with the sea surface temperature at the ship's location. Calculated values of  $C_N^2$  average a factor of 4 times the optically measured values. This is completely different than the results for the equilibrium cases. The explanation is as follows: at the ship the elevated sea surface temperature is measured which results in a large calculated  $C_N^2$  due to the large air-sea temperature difference. However, the thermal turbulence in the air is significantly influenced by the temperature difference further upwind. How large the calculation will be in error depends on the time the surface layer has to adjust to the new temperature.

Further supporting evidence for this effect was obtained by the aircraft measurements of  $C_T^2$ , (Figure 3). From 25 km at

sea to the region of the optical beam  $C_T^2$  is fairly constant then rising about 70% closer to shore. The thermal turbulence does not respond instantly to the temperature change, as was suggested in the preceding paragraph.

The final conclusion concerning the bulk model is that it works quite well for predicting optical scintillation for an equilibrium surface layer. In non-equilibrium situations, the calculation can be expected to be in error, with the maximum error depending on the magnitude of local mean parameter discontinuities. In the open ocean, where surface temperatures tend to be horizontally uniform, the non-equilibrium situations are expected to be uncommon.



## V. THERMAL TURBULENCE MEASUREMENTS

As was indicated in Section II, measurements of thermal, wind speed, and water vapor turbulence were made during MAGAT. These data are used to calculate the scaling parameters  $T^*$ ,  $U^*$ , and  $q^*$  and the structure functions  $C_T^2$ ,  $C_q^2$ , and  $C_U^2$ . These parameters are related through Eqs 2 for T and q and similarly for U:

$$C_U^2 = U_*^2 z^{-2/3} g(\xi). \quad (11)$$

Traditionally one uses the rate of velocity turbulence dissipation,  $\epsilon$ , rather than  $C_U^2$ , and they are related by:

$$C_U^2 = 2.0 \epsilon^{2/3}. \quad (12)$$

The dissipation stability function,  $\phi(\xi)$ , is introduced to directly relate  $U_*$  and  $\epsilon$  as (8)

$$\epsilon = \frac{U_*^3}{\kappa z} \phi(\xi) \quad (13)$$

Turbulence signals are analyzed in two ways: (1) spectral analysis and (2) obtaining the rms of spatially or frequency filtered signals. The spectral method is based upon the assumption of the "local isotropy" and the Kolomogorov -5/3 slope of the one-dimensional power spectral density,  $F_x(k)$

$$F_x(k) = 0.25 C_x^2 k^{-5/3}, \quad (14)$$

where  $k$  is the wavenumber and  $x$  refers to  $T$ ,  $U$ , or  $q$ . Performing a Fourier spectrum analysis in the frequency domain ( $f$ ) and using Taylor's hypothesis gives:

$$C_x = 4 \left( \frac{2\pi}{U} \right)^{2/3} f^{5/3} F_x(f). \quad (15)$$

Using two sensors spaced a distance  $d$  apart, the structure function can be found by measuring the variance of the difference in  $x$

$$C_x^2 = \overline{[x(r) - x(r + d)]^2} / d^{2/3}. \quad (16)$$

If frequency filtering rather than the spatial filtering is used with upper and lower frequency limits,  $f_u$ ,  $f_l$ , then

$$\int_{k_l}^{k_u} F_x(k) dk = \overline{x'^2} = (x'_{rms})^2. \quad (17)$$

$f$  and  $k$  are again related through Taylor's hypothesis. Using Equ. 15, the structure function is related to the rms signal by

$$C_x^2 = \frac{8}{3} \left( \frac{2\pi}{U} \right)^{2/3} \frac{(x'_{rms})^2}{(f_l^{-2/3} - f_u^{-2/3})} \quad (18)$$

These analyses only apply in the inertial subrange so that the probe spacing for the spatial filtering technique and the frequency band for the frequency filtering technique must insure that only this range is included.

Measurements of  $C_T^2$  by microthermal sensors are very difficult because of the problem of salt loading. This is due to the wires becoming sensitive to humidity fluctuations when they are salt encrusted (14)(15). Humidity fluctuations will falsely elevate  $C_T^2$  and, hence, the calculated  $C_N^2$ . Values of  $C_N^2$  calculated from the turbulence results are listed in Table 3 and plotted vs  $C_N^2$ -optical in Figures 4 and 5.

Figure 4 shows results for which no correction for the salt loading effect has been made and the comparison is very poor. In Figure 5, we show results where a correction has been made. We correct the data by using signals that occurred immediately after washing the wires. The comparison improves somewhat but is still poor.

If the thermal turbulence measurements could be made correctly, this method should be superior to the bulk model calculation since the small scale turbulence which is responsible for optical scintillation is being measured directly. However, the measurements are very difficult and subject to error. We do not believe that the technique can be made to perform as well as the bulk method.

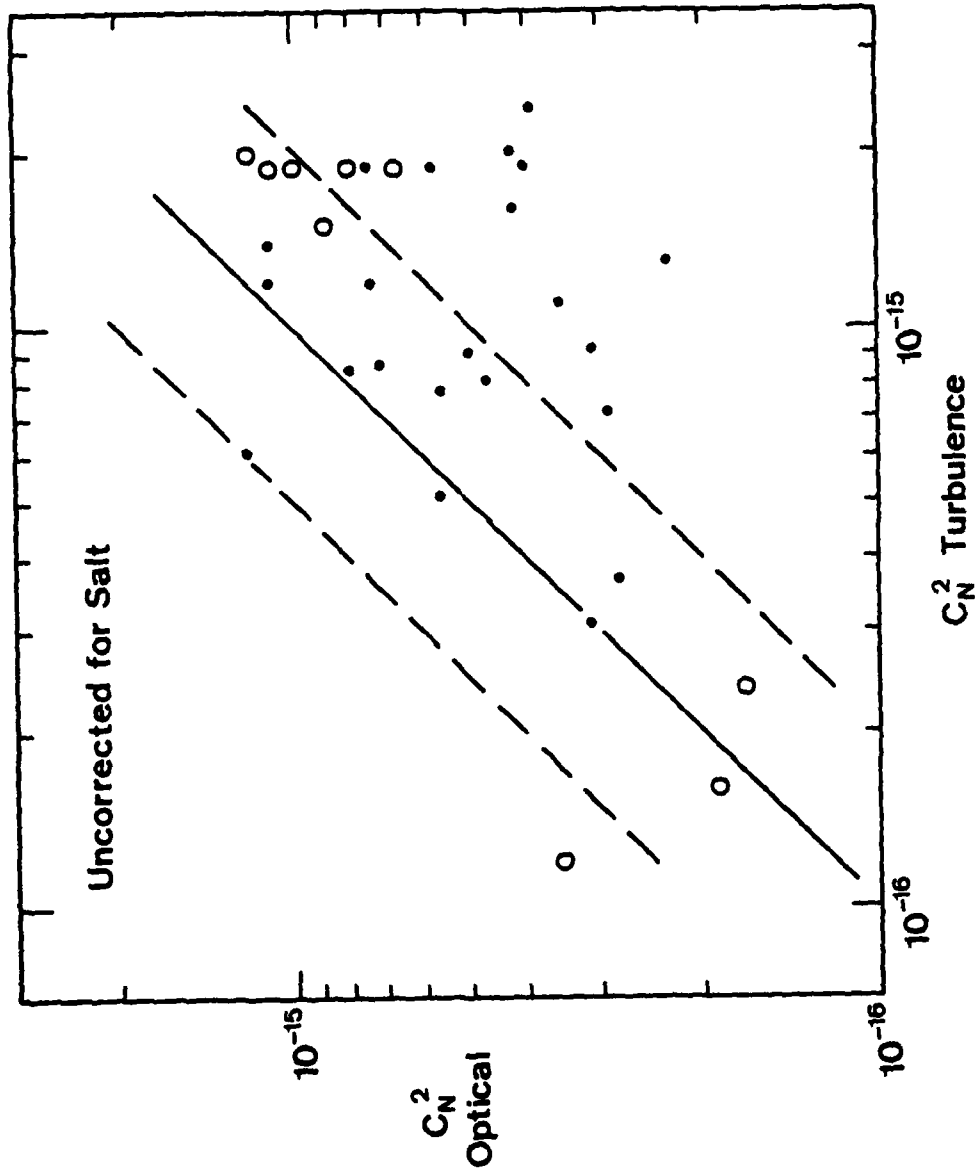


Figure 3

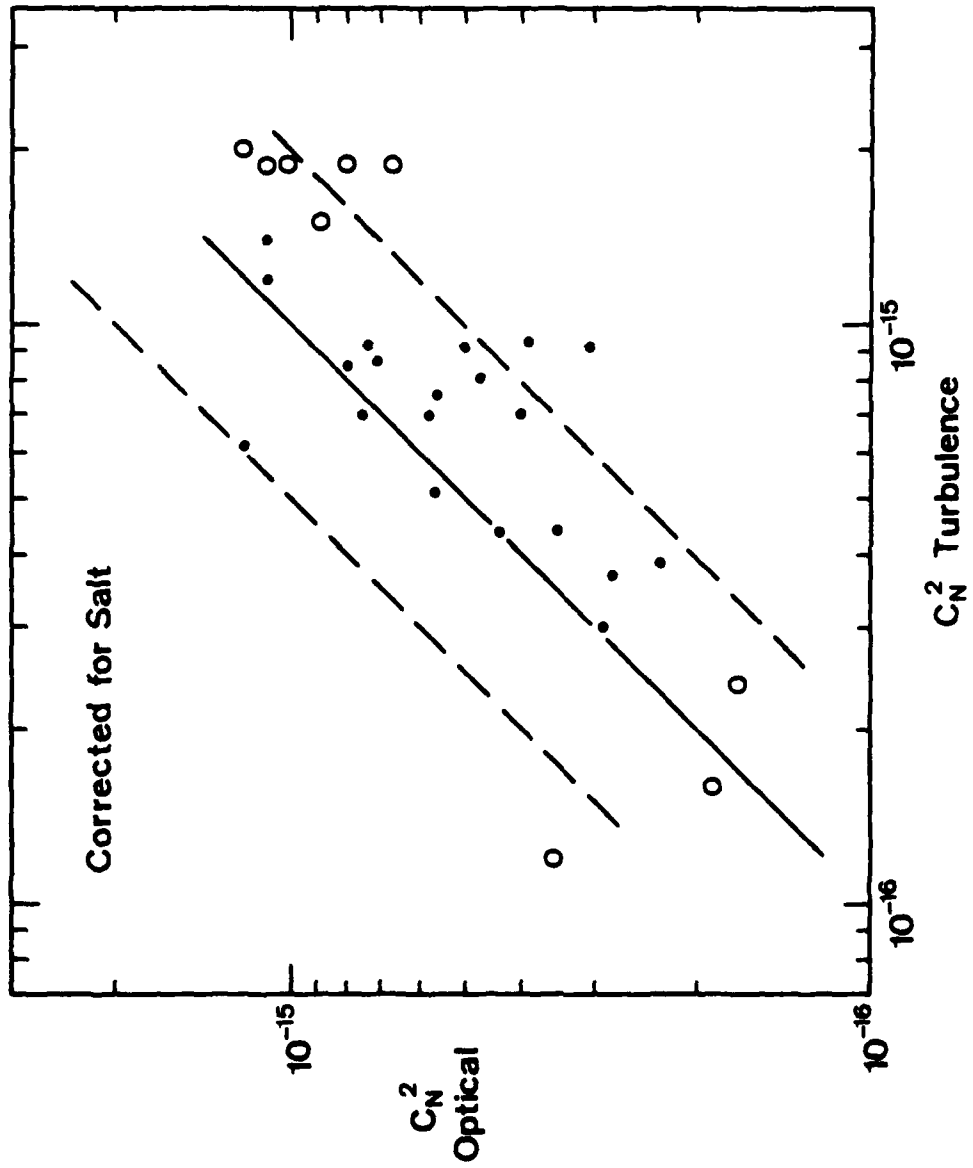


Figure 4

## VI. BULK MODEL WITH IR SEA SURFACE TEMPERATURE

Figure 6 shows a comparison of optically measured  $C_N^2$  and values calculated from the bulk model using the IR sea surface temperature. These results are not presented in tabular form. Obviously, there is very little agreement between measured and calculated values. (Three points are off the graph and not plotted.) This means that the bulk water temperature is a better measure of the surface temperature boundary condition for calculating surface layer fluxes.

This is a surprising result since the skin temperature, which is the parameter measured by an IR thermometer, should be the desired boundary condition. Note that in the bulk model the bulk calculation, including the stability, uses the IR temperature so that it is self consistent.

We have compared the IR and bulk temperature directly to see if there is a systematic error or some environmental effect. It is normal procedure before every cruise to calibrate all temperature sensors in the laboratory to insure that they read the same. This was done for MAGAT, including the IR thermometer. A water bath with an immersed platinum thermometer was used for the IR calibration. The two temperatures did not differ by more than  $0.3^\circ\text{C}$  from  $0^\circ\text{C}$  to  $40^\circ\text{C}$ , and the differences could be accounted for by difficulties in mixing the water to ensure the bulk and surface were in equilibrium. We are confident that any difference in bulk and IR temperatures measured at sea are not instrument problems.

In Figure 7, we show the measured temperature difference, IR-bulk, as a function of time. Gaps in the data appear for

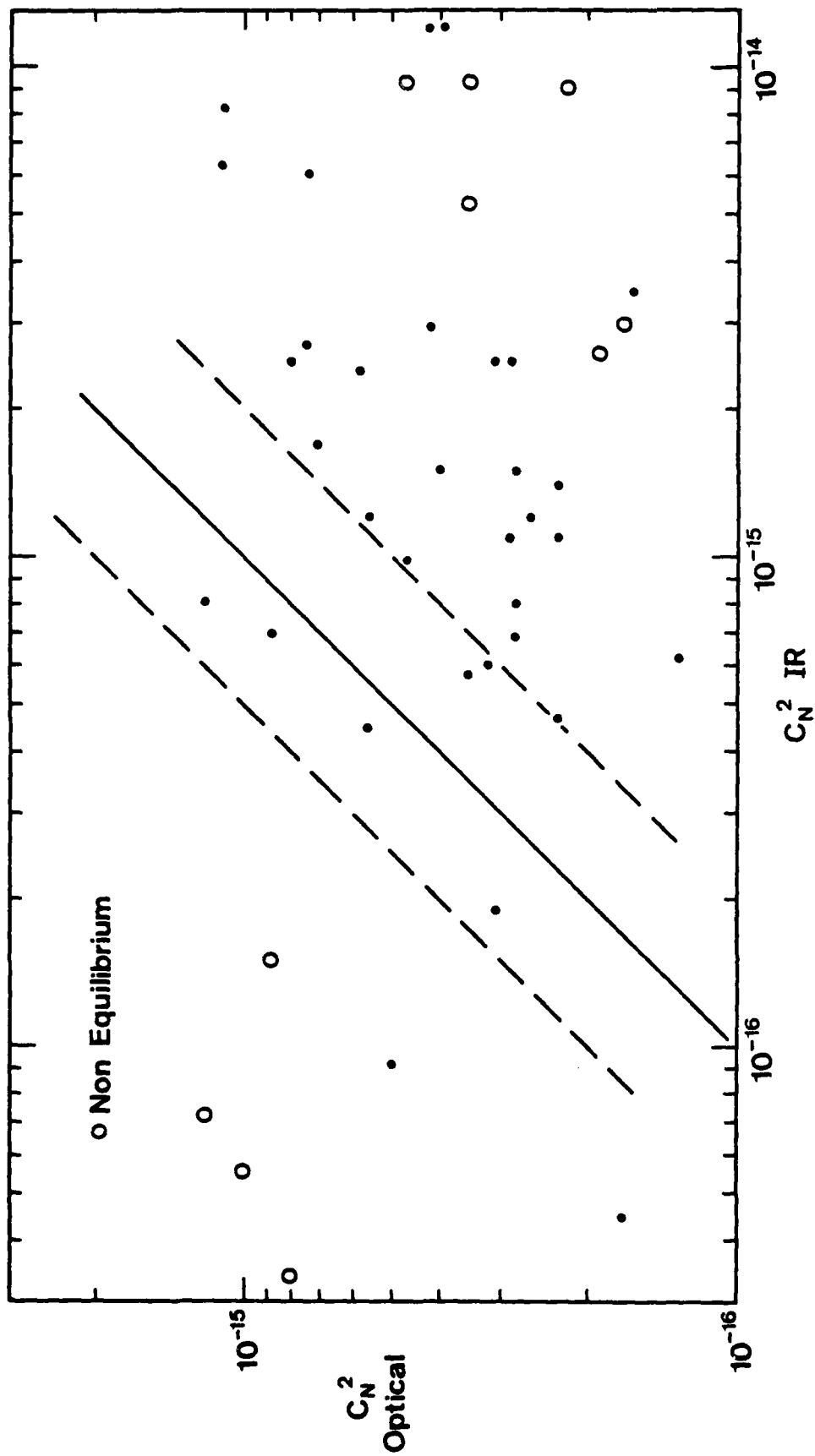


Figure 5

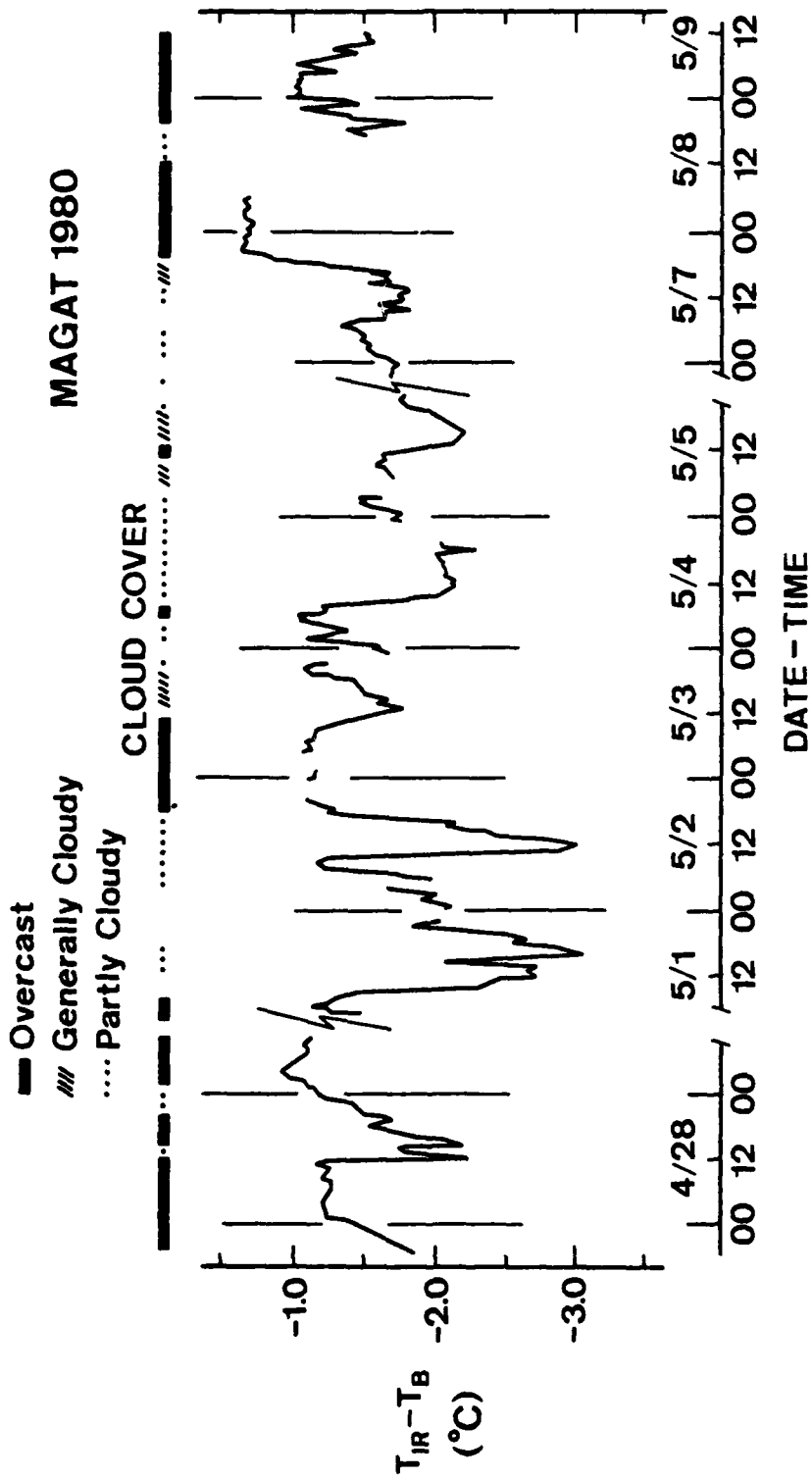


Figure 6

times when the ship was at the dock or the measurement system was turned off. The IR temperature is always lower than the bulk, which is consistent with observations that we have made on all previous cruises. The temperature difference varies from  $-0.6^{\circ}\text{C}$  to  $-3^{\circ}\text{C}$ .

We have checked several parameters to attempt to find a correlation with the difference: wind speed, swell and wave heights, ship location, ship speed, bulk temperature, and insolation. No correlation has been found except for an indirect correlation with insolation. The correlation is indirect because we did not measure insolation and only infer it from time of day, with which the IR temperature shows a correlation. However, the possible insolation correlation is opposite to what should occur since absorption of solar radiation would raise the skin temperature with respect to the bulk.

In Fig. 7 we also show a rough schematic representation of the cloud cover. The temperature difference is lowest when the skies are overcast. This effect can be accounted for by reflection of the cloud radiance off the sea surface for which a correction can be applied. The effect of such a correction would be to increase the temperature difference, removing some of the fluctuations but not the difference.

Results from Wesely<sup>(16)</sup> measuring IR and bulk temperatures on a calm cooling pond show temperature differences from 0.3 to  $1.5^{\circ}\text{C}$  with water temperatures varying from 0 to  $40^{\circ}\text{C}$ . The effect should be smaller for a wavy surface. Apparently, we cannot explain our results on the basis of the heat transfer rate

through the thermal skin.

As of this time, we do not know why the IR temperature is as much as 3°C lower than the bulk. In order to utilize the bulk model, the bulk water temperature must be used until an appropriate correction to make to radiation temperatures can be found.

## VII CONCLUSIONS

The NPS bulk aerodynamic model for calculating the optical index of refraction structure function,  $C_N^2$ , works quite well. It can be expected to predict  $C_N^2$  to within 50% for homogeneous, open ocean conditions. In coastal areas where strong local gradients exist, errors as large as a factor of 10 could result if meteorological data is obtained near the gradient. Weather fronts can also be expected to produce errors but there the gradients will be much weaker.

The appropriate sea surface temperature to use in the bulk model is the bulk water temperature averaged over the first few inches below the surface. Temperature measured by an IR thermometer cannot be used directly in the bulk model. The small scale turbulence in the atmospheric surface layer, which is in direct response to air-sea transfers of heat and momentum, appears to be in thermal equilibrium with the bulk water rather than the surface water film.

#### REFERENCES

1. E.C. Crittenden, A. Cooper, E. Milne, W. Rodeback, R. Armstead and S. Kalmbach, NPS 61-78-006.
2. E.C. Crittenden, et.al., "Overwater optical scintillation measurements during MAGAT-1980," report in preparation.
3. C.W. Fairall, G.E. Schacher, K.L. Davidson, and T.M. Houlihan, NPS report NPS61-78-007, (Sept. 1978).
4. K.L. Davidson, T.M. Houlihan, C.W. Fairall, and G.E. Schacher, Bound. Layer Meteor., 15 507-523 (1978).
5. C.W. Fairall, G.E. Schacher, and K.L. Davidson, "Measurements of the Humidity Structure Function Parameters,  $C_q^2$  and  $C_{Tq}$ , over the Ocean", Bound. Layer Meteor., to be published.
6. G.E. Schacher, K.L. Davidson, and C.W. Fairall, "Measurements of the Rate of Dissipation of Turbulent Kinetic Energy,  $\epsilon$ , Over the Ocean", Bound. Layer Meteor., to be published.
7. C.A. Friehe, Appl. Optics, 16, 334 (1977).
8. J.C. Wyngaard, YU. Izumi and S.A. Collins, J. Opt. Soc. Am. 61, 1646 (1971).
9. J.C. Wyngaard, "Workshop on Micrometeorology", AMS publication (Science Press, Ephrates, PA, 1973) p. 127.
10. J.A. Businger, "Workshop on Micrometeorology", AMS publication (Science Press, Ephrata, PA, 1973) p. 76-77.
11. J.A. Businger, J.C. Wyngaard, Y. Izumi and E.F. Bradley, J. Atmos. Sci. 28, 181 (1971).
12. J.R. Garratt, Monthly Weather Review, 105, 915 (1975).
13. J. Kondo, Bound. Layer Meteor., 9, 91 (1975).
14. C.W. Fairall, K.L. Davidson, and G.E. Schacher, J. Appl. Meteor. 18, 1237 (1979).
15. K.F. Schmitt, C.A. Friehe, and C.H. Gibson, J. Phys. Oceanogr. 8, 115 (1978).
16. M.L. Wesely, J. Geophysical Research 84, 3696 (1979).

DISTRIBUTION LIST

	No. of Copies
1. Defense Documentation Center Cameron Station Alexandria, Virginia 22314	2
2. Library, Code 0142 Naval Postgraduate School Monterey, California 93940	2
3. Dean of Research, Code 012 Naval Postgraduate School Monterey, California 93940	1
4. Dr. C.W. Fairall BDM Corporation, 1340 Munras St. Monterey, California 93940	4
5. Professor J. Dyer, Code 61Dy Naval Postgraduate School Monterey, California 93940	1
6. Professor G.J. Haltiner, Code 63Ha Naval Postgraduate School Monterey, California 93940	1
7. Assoc. Professor K.L. Davidson, Code 63Ds Naval Postgraduate School Monterey, California 93940	10
8. Professor G.E. Schacher, Code 61Sq Naval Postgraduate School Monterey, California 93940	4
9. Professor E.C. Crittenden, Code 61Ct Naval Postgraduate School Monterey, California 93940	1
10. Lt. Gary Ley PMS-405 Naval Sea Systems Command Washington, D. C. 20360	1
11. Dr. A. Goroeh Naval Environmental Prediction Research Facility Monterey, California 93940	1
12. Dr. A. Weinstein Director of Research Naval Environmental Prediction Research Facility Monterey, California 93940	1

13. Dr. Richard Lipes 1  
Mail Stop 238-420  
Jet Propulsion Laboratory  
4800 Oak Grove Drive  
Pasadena, California 91103
14. Dr. Kristina Katsaros 1  
Atmospheric Sciences Dept.  
University of Washington  
Seattle, Washington 98195
15. Dr. C.A. Friehe 1  
Deputy Manager for Research, RAF  
National Center for Atmospheric Research  
P.O. Box 3000  
Boulder, Colorado 80307
16. Dr. J.C. Wyngaard 1  
CIRES  
University of Colorado/NOAA  
Boulder, Colorado 80309
17. Dr. Marvin L. Wesely 1  
Radiological and Environmental Research Division  
Argonne National Laboratory  
Argonne, Illinois 60439
18. Dr. Owen Cote 1  
ESD/WE  
Stop 7  
Hanscom AFB, Massachusetts 01731
19. Dr. Hans Panovsky 1  
Department of Meteorology  
Penn State University  
State College, Pennsylvania
20. CDR K. Van Sickle 1  
Code Air-370  
Naval Air Systems Command  
Washington, D. C. 20360
21. Dr. A. Shlanta 1  
Code 3173  
Naval Weapons Center  
China Lake, California 93555
22. Dr. Barry Katz 1  
Code R42  
Naval Surface Weapons Center  
White Oak Laboratory  
Silver Spring, Maryland 20362

23. Dr. J.H. Richter 1  
Code 532  
Naval Oceans Systems Center  
San Diego, California 92152
24. Dr. Lothar Ruhnke 1  
Code 8320  
Naval Research Laboratory  
Washington, D.C. 20375